Rare Metal Materials and Engineering
Volume 49, Issue 5, May 2020
Available online at www.rmme.ac.cn

Science Press

Cite this article as: Rare Metal Materials and Engineering, 2020, 49(5): 1483-1490.

ARTICLE

Visualization and Numerical Simulation of Material Flow in Al/Mg Dissimilar Friction Stir Welding

Song Bo[1], Zhai Yangyang[1], Zuo Dunwen[2], Deng Yongfang[3]

[1] Lanzhou University of Technology, Lanzhou 730050, China; [2] Nanjing University of Aeronautics and Astronautics, Nanjing 210016, China; [3] Jiangxi University of Science and Technology, Ganzhou 341000, China

Abstract: The flow mode of materials is closely related to the formation of joint structure, which has a crucial influence on the mechanical properties of joints for friction stir welding (FSW). The material flow of the joint was studied by slicing method which was adopted to observe different layers of dissimilar friction stir butt welding. The visualization of the material flow was accomplished by 3D reconstruction of the joint, which shows the flow pattern of the joint and the cause of the defect. The three-dimensional mathematical model of the flow of Al/Mg materials in FSW process was established based on computational fluid dynamics (CFD) and multiphase flow theory. The material flow patterns were analyzed and predicted under different welding parameters by the distribution of tracing particles added in numerical models. Results reveal that the flow of material in the upper part of the joint is strong, and the material moves to the front of tool as a whole. The magnesium alloy in the middle part in the advancing side of the joint moves forward to the front of the tool, and the temporarily cavity is filled with aluminum alloy from the retreating side. The cavity which is not completely filled will form a hole defect when the material flow is insufficient due to improper process parameters. The whole joint material is mainly laminar flow. The flow mode of joint material is basically unchanged when the heat input is satisfied. The transfer distance and mixing mode of material will change under the condition of high rotation speed or overheat. The two materials cross the butt line for many times in the mode of laminar flow around the tool and are fully mixed when the turbulence occurs on the retreating side.

Key words: dissimilar friction stir welding; 2024 aluminum alloy; AZ31 magnesium alloy; plastic materials flow; numerical simulation

The increasing attention of energy conservation and environmental protection has raised researcher's awareness of utilizing lightweight materials in industry. Aluminum alloy and magnesium alloy are good examples. The lightweight materials with low density, high specific strength and good anti-corrosion properties have become an important part of lightweight aerospace, high-speed trains, and other modern transportation vehicles. With the burgeoning of science and technology, joining of dissimilar materials is highly required. The traditional aluminum and magnesium alloy joining technology has many problems, since intermetallic compounds produced at high temperatures will seriously affect the performance of joints[1-3].

Friction stir welding (FSW) is patented by The Welding Institute (TWI) in 1991, which is a solid phase connection technology derived from the traditional friction welding, and has become an important and conventional joining process for light alloy[4,5]. Since its invention, FSW has been widely analyzed both experimentally and simulatively[6-8]. However, Because of the characteristics of FSW, it is difficult to directly observe the flow of the material. The internal material flow of FSW is different from that of other welding modes, especially for dissimilar materials[8]. The material flow mode is very complicated in the process of FSW, and the distribution of the material in the stirring zone varies with the distance from the shoulder[9]. The ma-

Received date: May 21, 2019
Foundation item: Natural Science Foundation of Gansu Province (18JR3RA146, 18JR3RA147)
Corresponding author: Song Bo, Ph. D., School of Mechatronic Engineering, Lanzhou University of Technology, Lanzhou 730050, P. R. China, E-mail: topsb1983@163.com

terial flow pattern depends on the nature of the material being joined, the material and the shape of the tool as well as the contact and position with workpiece[2]. Larsson et al[10] studied the flow of materials of the butt FSW for dissimilar materials. The results show that the microstructure of dissimilar FSW joint is very similar to that of typical FSW joints. In the FSW of aluminum and magnesium alloy, the mechanical lock structure is the most common macroscopic phenomena[11]. Li Ying et al[12] showed that the material flow behavior of dissimilar FSW is complex. The metal flow path can be visualized because of the two different metal corrosion resistances. Therefore, understanding material flow during FSW is crucial for controlling the weld quality, especially for different process parameters.

Material flow during FSW of 3.2 mm thick 2024 aluminum alloy and AZ31 magnesium alloy sheets using different process parameters was investigated by experimentation and modeling. In the first part, the joint slicing method was used to realize the visualization of material flow. In the second part, numerical analysis based on the CFD theory was used to analyze the material flow pattern and compared with the experimentally measured values.

1 Flow Visualization Experiments

1.1 Experimental method

The materials used in this work were 2024 aluminum alloy and AZ31 magnesium alloy plates with a thickness of 3.2, 200 mm in length along the welding line, and 100 mm in width on each side. Dissimilar FSW were performed using FSW-3LM-015 FSW machine with a tilt angle of 3°. The section method 1 (M1) of joint is shown in Fig.1a, where aluminum alloy and magnesium alloy are placed on the retreating side and advancing side, respectively. The section method 2 (M2) of joint is shown in Fig.1b, where the placing position is opposite to the former. The strength joint placed using the two ways of placing method is very close. The process parameters and the size of the tool are shown in Table 1.

In order to study the plastic flow behavior of the joint metal, the middle part of the joint was selected as two samples, and the two samples were ground and polished from two directions. The joint M1 cross section is perpendicular to the feed direction, as shown in Fig.1a. The magnesium alloy of joint was chemically etched after polishing, then observed and photographed under the optical microscope. The pixels of image were identified for all sections of M2 method in the Photoshop software to determine the interface of the two kinds of metals, and then the 3D visualization of joint was realized.

Table 1 Process parameters for FSW experiment

Parameter	Value
Rotation speed, ω/r·min^{-1}	500
Feed speed, v/mm·min^{-1}	500
Tool shoulder diameter, R/mm	15
Pin root diameter, R_1/mm	4
Pin head diameter, R_2/mm	3

1.2 Material flow in the direction of the joint cross section

Fig.2 shows the images of the cross section after chemical corrosion. The white solid line indicates the original interface of the butt joint, the center line of the tool, and the outline of the pin. As shown in Fig.2, The TMAZ can be observed obviously on the aluminum alloy side, and a large amount of magnesium alloy is transferred to the aluminum side of the joint on the upper cross section and some magnesium is even into the aluminum alloy due to the movement of pin root. A part of the aluminum alloy is "squeezed" into the section of the magnesium alloy. The material is transferred within the scope of shoulder. The transfer of the upper material is mainly caused by the action of the tool shoulder. A lot of heat is generated between the shoulder and joint surface, softening the advancing side (AS) and retreating side (RS) materials on the upper surface of the joint. The transfer phenomenon of a large number of materials occurs under the action of friction force and material viscosity. Material transfer is not very obvious in the middle of the joint, only a small amount of material transfer. Material is transferred into the aluminum alloy substrate because of the pin effect at the bottom of the joint, and the transferred material and magnesium alloy substrate are continuous. The transfer makes the joint form a "mechanical locking" structure, which increases the strength of the joint between aluminum and magnesium.

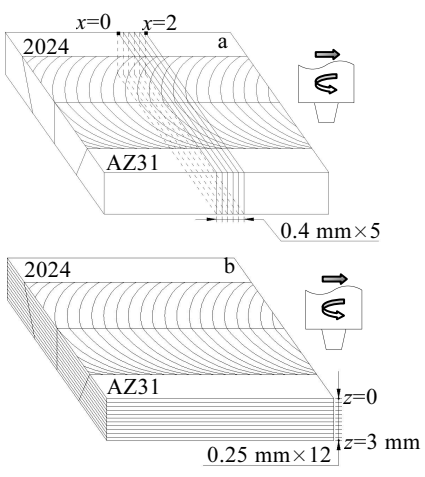

Fig.1 Schematic of the joint section: (a) perpendicular to feed direction and (b) parallel to feed direction

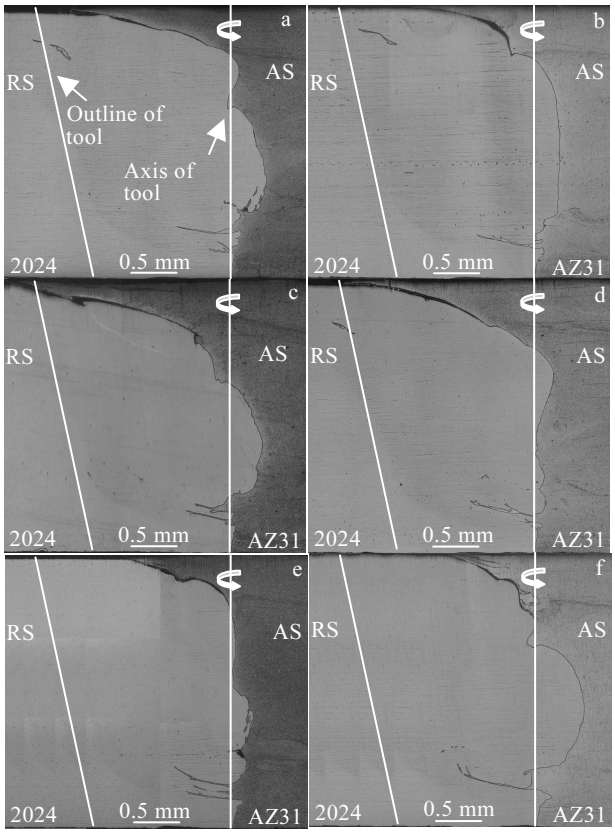

Fig.2 Cross section images of different positions in welding direction: (a) x=0, (b) x=0.4 mm, (c) x=0.8 mm, (d) x=1.2 mm, (e) x=1.6 mm, and (f) x=2.0 mm

1.3 Material flow in the direction of joint surface

In order to understand the flow of plastic metal in the horizontal direction, the image was obtained from the surface to bottom of the joint. The upper, middle and bottom part of the joint are selected as the representative 3 pictures.

Fig.3 shows an image of the etched joint on the top surface of the workpiece. The transport of the topmost material is more affected by the bottom of the tool shoulder. Under the action of rotating tool, a substantial amount of aluminum alloy which is located in the retreating side is transported to the back of the tool, leaving an image where aluminum alloy generally points to the tangent direction of the outer edge of the shoulder. Two kinds of material is basically continuous, and aluminum alloy zigzag outer edge is sharp and serrated edge of magnesium alloy is blunter. Because of the difference of Al/Mg alloy plasticity, it can be inferred that metal flow caused by the mutual extrusion between materials on the surface of the joint under the shoulder is more significant. Aluminum material flows to the magnesium alloy side, and the magnesium alloy is affected by the action of the shoulder and the aluminum alloy extrusion flowed to the direction of the red arrows shown in Fig.3. Material generally flows from the advancing side to the retreating side, and then accumulates layer by layer in the case of sufficient plastic metal flow in FSW joint [13]. However, this is not the case in Fig.3. The metal flow on the most superficial surface of joint is not sufficient, which may be due to the small ratio of rotation speed and feed speed.

Fig.4 shows images of the middle part of etched joint. The zigzag shape is regular and the two sides of the joint are symmetrical. The distance between each saw tooth is exactly the ratio of rotation speed and feed speed, which is 1 mm. This shows that a saw tooth forms and materials complete a buildup when the tool rotates a circle. This is also one cycle of material flow period. There is a small amount of aluminum alloy between each saw tooth on the advancing side of magnesium alloy, which means that the degree of metal flow to each other on the advancing side and retreating side is not very strong or too late to transport further at a lower ratio of rotation speed and feed speed. The stir effect of tool is gradually weakened from the surface to the bottom of joint because the pin is a taper, which gradually decreases the transport volume of the plastic metal of aluminum alloy compared with the upper layer.

As shown in Fig.5, hole defect gradually appears in the joint, which is located on the aluminum side of the Mg/Al initial butt interface starting from z=2 mm to the bottom. The magnesium alloy is transported from the advancing side to the retreating side and piled up at the back of the tool eventually. In this continuous dynamic process, the hole are formed temporarily since transferred magnesium alloy is not backfilled sufficiently by aluminum alloy located on the retreating side, so as to cause the formation of hole defect. There is no hole in the right side of the image, which shows that the holes are filled with aluminum alloy, and some of the metal moves into the advancing side of magnesium alloy. This may be due to the deformation of the plate during the welding process, increasing the plunge depth of shoulder indirectly.

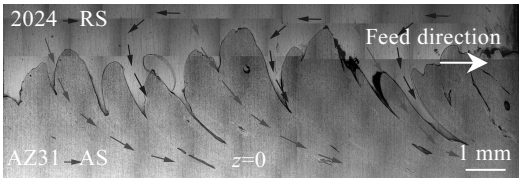

Fig.3 Surface layer section diagram of the etched joint at z=0

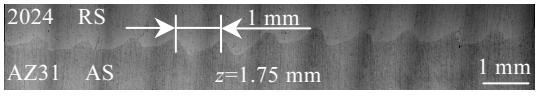

Fig.4 Middle layer section diagram of the etched joint at z=1.75 mm

Fig.5 Bottom layer section diagram of the etched joint at z= 2.5 mm

1.4 Material flow visualization of Mg/Al dissimilar FSW joint

Fig.6 was produced by extracting the pixel positions from each digital image, similar to Fig.3. The pixel position becomes x and y coordinates of a given point and the z coordinate is determined by the height in the joint, from which the image can be obtained.

In Fig.6, a large amount of aluminum alloy is transported in the surface layer of the joint. In the middle of the joint, the magnesium alloy in wave is transported into the aluminum alloy side. The hole defect like black spot appears in the lower part of the joint. From Fig.6, it can be assumed that the material mainly affected by the shoulder moves into the advancing side and the material mainly affected by the pin moves into the retreating side[14]. Meantime, there is a material rise every 1 mm in the forward direction due to the ratio of feed and rotation speed, and the time when the tool rotates a circle is a cycle of joint formation. Due to the rotation and the eccentric motion around the spindle of the tool, the flowing material can accumulate at the back of the tool with its feed movement. It is not obvious that the plastic metal material flows from the top to the bottom of joint at 500/500 process parameter through 3D reconstruction image. Materials have a strong liquidity affected by the rotation shoulder relative to pin. So, the plastic metal flow of FSW joint is a complex turbulent flow phenomenon. Although 3D reconstruction image does not present the process information of material flow, it can be inferred that the material transfer is completed in a period of joint accumulation because of the low ratio of feed and rotation speed and fast feed speed.

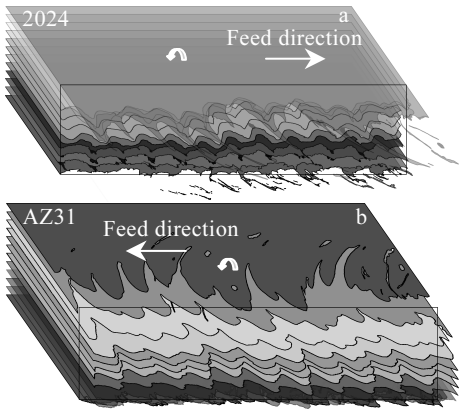

Fig.6 3D reconstruction of joint surface sections: (a) aluminum side and (b) magnesium side

2 Numerical Analysis of Plastic Material Flow

The joint slicing technique and visualization cannot directly provide detailed information about the actual flow field of the material because it only shows the final position of the mark in the weld. Mathematical modeling is a powerful tool to quantitatively describe the heat transfer and material flow during FSW.

The application of fluid mechanics based model requires a viscosity function to simulate the material flow behavior of dissimilar friction stir welding. The FSW process is modeled using different material constitutive equations. First, a constant, high Newtonian viscosity is assumed. No simulation can capture FSW like flow pattern. It is, therefore, obvious that only a temperature and deformation rate (strain rate) dependent viscosity can sufficiently describe the "true" rheological properties of the alloy at elevated temperatures and high deformation rate.

The temperature and strain rate dependent dynamic viscosity μ can be calculated from flow stress and effective strain rate as follows[15]:

$$\mu = \frac{\sigma}{3\bar{\dot{\varepsilon}}} \tag{1}$$

where $\bar{\dot{\varepsilon}}$ is effective strain rate and σ is flow stress.

The effective strain rate is determined by Zener-Hollomon equation as follows[16,17]:

$$\dot{\varepsilon} = A\exp\left(-Q/RT\right) \tag{2}$$

where Q is the temperature-independent activation energy, R is the gas constant, and A is the material constant; Z is the Zener-Hollomon parameter which represents the temperature compensated effective strain rate and is calculated according to Eq.(3):

$$Z = \dot{\varepsilon}\exp\left(-Q/RT\right) \tag{3}$$

Based on the Zener-Hollomon formula, Sellers and Tegart et al[18] joined the strain rate sensitivity factor, and got Eq.(4):

$$\dot{\varepsilon} = A\exp\left(-Q/RT\right)\left[\sinh\left(\alpha\sigma\right)\right]^{1/m} \tag{4}$$

where m and α are material constants, if n=1/m.

Combining Eq.(1~4), the viscosity can be expressed as follows:

$$\mu = \frac{1}{3\alpha\bar{\dot{\varepsilon}}}\ln\left\{\left(Z/A\right)^{1/n} + \left[\left(Z/A\right)^{2/n} + 1\right]^{1/2}\right\} \tag{5}$$

The two alloys shown in Table 2 were used in the present research. The material constant of 2024 and AZ31 was taken from Ref.[19].

All the parameters are taken to Eq.(5), and visco-plastic constitutive equation of 2024 and AZ31 can be obtained as follows:

$$\mu_{2024}=\frac{24.06}{\dot{\varepsilon}}\ln\left\{\begin{bmatrix}\left[\dot{\varepsilon}*\left(\exp\frac{28143.67}{T}-34.28\right)\right]^{0.2165}+\\ \left[\left(\dot{\varepsilon}*\left(\exp\frac{28143.67}{T}-47.8\right)\right)^{0.4329}+1\right]^{0.5}\end{bmatrix}\right\} \quad (6)$$

$$\mu_{\mathrm{AZ31}}=\frac{71.28}{\dot{\varepsilon}}\ln\left\{\begin{bmatrix}\left[\dot{\varepsilon}*\left(\exp\frac{30334.82}{T}-47.8\right)\right]^{0.1095}+\\ \left[\left(\dot{\varepsilon}*\left(\exp\frac{30334.82}{T}-47.8\right)\right)^{0.219}+1\right]^{0.5}\end{bmatrix}\right\} \quad (7)$$

Table 2 Material constants of 2024 and AZ31 alloys for the viscosity calculation in Eq.(4) and Eq.(5)

Alloy	α/Pa^{-1}	Q/J·mol^{-1}	A/s^{-1}	n
2024	0.024	234000	7.72e14	4.62
AZ31	0.0081	252218	5.718e20	9.13

The data related to the material properties used in the calculation such as the specific heat (C_p) and thermal conductivity (λ) are investigated by STA-409CD thermal analyzer and TC-7000H laser thermal conductivity instrument.

$$C_{\mathrm{p2024}}=\begin{cases}642.63+1.11T-0.0013T^2+7.76\mathrm{e}-7T^3 & T=298\sim748\ \mathrm{K}\\ -1.12\times10^6+4243.03T-5.74T^2+0.0023T^3 & T=748\sim847\ \mathrm{K}\end{cases} \quad (8)$$

$$C_{\mathrm{pAZ31}}=997.16+0.25T+2.65\mathrm{e}-4T^2 \quad T=298\sim847\ \mathrm{K} \quad (9)$$

$$\lambda_{2024}=87.42+0.11T-3.06\mathrm{e}-6T^2-3.06\mathrm{e}-8T^3 \quad T=298\sim873\ \mathrm{K} \quad (10)$$

$$\lambda_{\mathrm{AZ31}}=92.26-0.0064T-6.81\mathrm{e}-5T^2 \quad T=298\sim873\ \mathrm{K} \quad (11)$$

The material density (ρ) of 2024 and AZ31 is 2674 and 1698 kg/m^3, respectively. The material flow should meet the following conservation equations:

$$\nabla u=0 \quad (12)$$

$$\rho u\cdot\nabla u=-\nabla p+\mu\nabla^2 u \quad (13)$$

$$\rho c_p u\cdot\nabla u=\lambda\nabla^2 T+Q_{\mathrm{vd}} \quad (14)$$

where u is the velocity vector, p is the static pressure and Q_{vd} is the internal heat source term.

It is assumed that frictional heating is the heat source and friction coefficient can be estimated. Milling and Grong[20] estimated the heat input in friction welding by the torque and angular velocity assuming a constant friction coefficient. Using the apparent similarity between friction welding and FSW and assuming a uniform pressure distribution under the FSW tool shoulder and pin, the heat generation can be estimated. If frictional heating occurs only at the tool shoulder, the heat input is calculated as follows:

$$\dot{Q}=\int\mu P\omega r\mathrm{d}A=\int_{r_0}^{r}\mu\frac{F_z}{A_s}\omega r2\pi r\mathrm{d}r=\mu\frac{2}{3}\frac{F_z}{A_s}\omega\left(r_s^3-r_0^3\right) \quad (15)$$

where $\dot{Q}$ is the net power, μ is the friction coefficient, P is the uniform pressure under the tool, ω is the angular velocity, r is the radius of shoulder, F_z is the vertical tool force and A_s is the shoulder area.

The welding heat is mainly generated through the friction of shoulder and material. Studies indicate that the result of temperature field simulation coincides with experiment when assuming that the heat produced by pin makes up 25% of total heat produced by the tool. Therefore, it is assumed that the pin accounts for 25% of the total heat production.

The model assumes that the material sticks to the tool surface, so the material velocity equals the rotation speed multiplied by the radius. The translation is prescribed by allowing the material to flow past the tool. Therefore, the material enters the model at a velocity equal to the welding speed at ambient temperature, as shown in Fig.7. The tool pin surface is assumed as an adiabatic rotating wall. The top and bottom of the flow domain are modeled as moving walls with convective heat transfer to the surroundings. Both walls move at the welding speed. The advancing and the retreating sides are set as moving walls and the moving speed is equal to the welding speed. For all other surfaces, the velocities and temperatures are set to zero and ambient temperature, respectively.

3 Results and Discussion

Fig.8 shows the particle tracking map for FSW at different process parameters using a tool with a shoulder diameter of 15 mm. Aluminum and magnesium materials are represented by red and blue particles, respectively. The position of tracer particles which are embedded is in the section of the inlet of the model material, as shown in Fig.8. The location of tracer particles is recorded on the picture when they move into the aluminum alloy side at the maximum distance. The transport distance of magnesium alloy and aluminum alloy flowing with the front of the tool moved into the aluminum alloy side changes little at rotation speeds of 500, 800 and 1000 r/min and feed speed of 500 mm/min. The range of stir zone and thermo-mechanically affected zone and joint morphology characteristics change

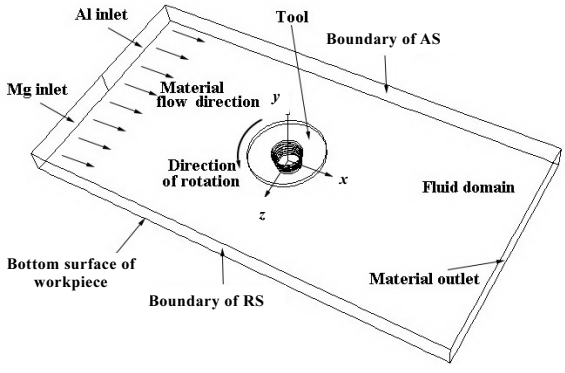

Fig.7 Schematic sketch of boundary conditions

little with the increase of the rotation speed at a low ratio of feed speed and rotation speed process parameter when the total transport of aluminum alloy is invariant. In general, the increase of the rotation speed has little effect on the flow pattern of joint when sufficient heat who can meet needs of material heat input can be generated by the tool at an adequate ratio of rotation speed and feed speed.

The transport distance to each side and mixing mode of the two materials are different at a high ratio of rotation speed/feed speed process parameter. Fig.9 is the particle tracking map at process parameter of 300/30. Fig.9b shows that the magnesium alloy is transferred into the advancing side and rotates with the tool continually when tool feeding distance is 6 mm at the 12th s. At the 36th s, magnesium and aluminum alloys are fully mixed, and the mixing position is deviated from the butt surface and located at the advancing side, as shown in Fig.9. On the advancing side, a large amount of magnesium alloy accumulates at rear of the tool and upper part of joint mainly, so it can be inferred that the effect of shoulder on the aggregation of magnesium alloy in the surface layer of the joint is very important.

The flow pattern of stir zone material is a thin material layer, which rotates with tool at high speeds. The larger velocity gradient, temperature gradient and stress gradient are generated near the tool, under the assumption that the surface of the tool is a non-sliding revolving wall. Guerra et al[21] observed the thin material layer rotating with the pin by pin-breaking technique. Fig.10 and 11 show the flow velocity contour at the upper-thickness and mid-thickness plane. The flow material is mainly driven by the rotation of the shoulder. It illustrates the influence of rotation speed on the material flow when the feed speed keeps constant. A higher rotation speed with greater line speed results in the increase of flow velocity of the material, close to the lateral line of the shoulder. The magnesium alloy should flow further to the advancing side when the feed speed keeps constant. But the reality is different. There is little difference in the morphology of the joint shown in Fig.8, which is due to the difference of the plasticity of the magnesium/aluminum. The material in upper joint flows downward on the advancing side due to the extrusion pressure in material when a large amount of material flows to the advancing side, because the viscosity of the magnesium alloy is lower relatively at the same temperature. As shown in Fig.11, the velocity of material flow on the side and the lower surface of the shoulder gradually decreases. The velocity gradient is larger on the advancing side so a rotational motion is formed in the middle of the joint. The material flow maldistribution occurs when the velocity gradient and stress gradient of the joint are large.

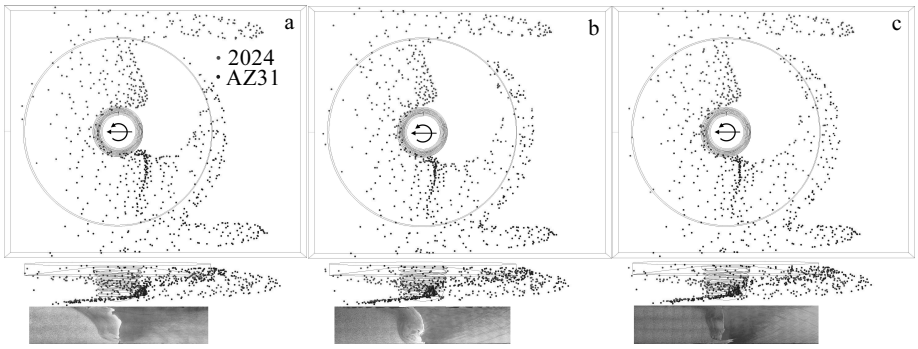

Fig.8 Particle tracking maps for FSW at different rotation speeds: (a) 500 r/min, (b) 800 r/min, and (c) 1000 r/min

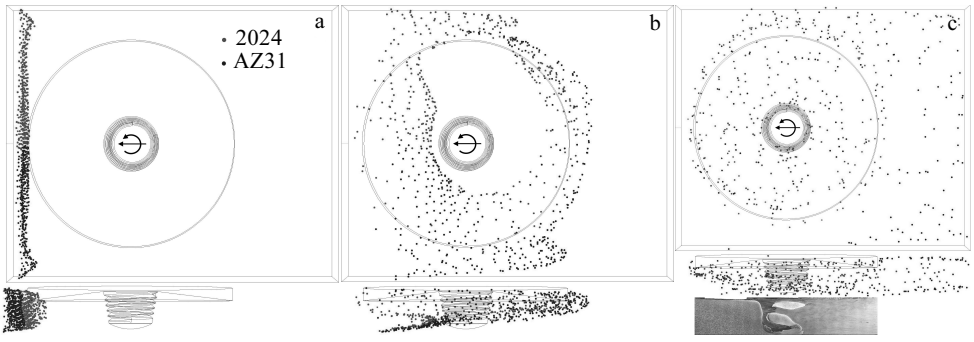

Fig.9 Particle tracking map for FSW at different time under a ratio of rotation speed/feed speed process parameter of 300/30: (a) 3 s, (b) 12 s, and (c) 36 s

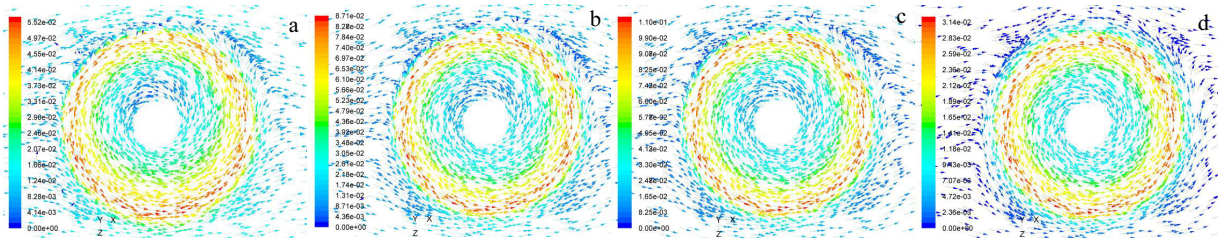

Fig.10 Velocity contour under different process parameters (y=2.2 mm): (a) 500/500, (b) 800/500, (c) 1000/500, and (d) 300/30

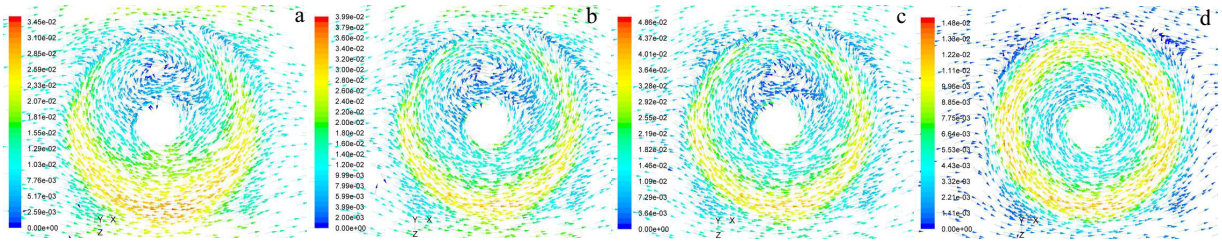

Fig.11 Velocity contour under different process parameters (y=1.6 mm): (a) 500/500, (b) 800/500, (c) 1000/500, and (d) 300/30

4 Conclusions

1) Using joint slicing technique and extracting the pixel to realize 3D reconstruction of joint, the general mode of the material flow during dissimilar friction stir welding of 2024 aluminum alloy and AZ31 magnesium alloy plates is examined and evaluated in metallographic ways.

2) The material mixing of magnesium alloy and aluminum alloy does not appear at a low ratio of feed and rotation speed process parameters. The material flow in the upper part of the joint is strong, and the material moves to the front of tool as a whole under the action of lower shoulder part. And the magnesium alloy of the middle part in the advancing side of the joint moves forward to the front of the tool. The cavity formed by the magnesium transfer is filled with aluminum alloy from the advancing side, thus forming a mechanical locking structure which increases the intensity of joint. The kinetic energy of material flow decreases gradually from the middle part to the lower part of the joint and the cavity cannot be filled completely because of the insufficient flow of the material.

3) A three-dimensional model is developed for numerical simulation of plastic material flow in friction stir welding of magnesium and aluminum alloy. The equations of conservation of mass, momentum and energy are numerically solved to quantitatively describe the visco-plastic flow of the material during the friction stir welding under different process parameters. The increase of the rotation speed has little effect on the flow pattern of joint when sufficient heat who can meet the needs of material heat input can be generated by the tool at an adequate ratio of rotation speed and feed speed.

4) The increase of rotation speed has little effect on the joint formation and the basic flow mode of the material when the sufficient heat meets the heat input requirements of the material under a proper ratio of rotation speed and feed speed, that is, laminar flow is the main pattern. The material transfer distance and mixing mode may change under high ratio of rotation speed and feed speed, that is, the two materials cross the butt line for many times in the mode of laminar flow around the tool and mix fully when the turbulence occurs at the retreating side.

References

1 Li Shujian, Zhan Lihua, Chen Rong *et al*. *Rare Metal Materials and Engineering*[J], 2016, 45(9): 2282

2 Nandan R, DebRoy T, Bhadeshia H K D H. *Progress in Materials Science*[J], 2008, 53(6): 980

3 Chen Y C, Nakata K. *Scripta Materialia*[J], 2008, 58(6): 433

4 Jataa K V, Semiatin S L. *Scripta Materialia*[J], 2000, 43(8): 743

5 Mishra R S, Ma Z Y. *Materials Science and Engineering*[J], 2005, 50(1): 1

6 Yan D Y, Shi Q Y, Wu A P *et al*. *Journal of Mechanical Engineering*[J], 2010, 46(16): 106

7 Song M, Kovacevic R. *Journal of Engineering Manufacture*[J], 2003, 217: 73

8 Zhao Yong, Lu Zhengping, Yan Keng *et al*. *Materials and Design*[J], 2015, 65(1): 675

9 DebRoy T, Bhadeshia H K D H. *Science and Technology of Welding and Joining*[J], 2010, 14(4): 266

10 Larsson H, Karlsson L, Stoltz S *et al*. J. *2nd International*

Symposium on Friction Stir Welding[C]. Gothenburg: Mendeley, 2000
11 Liu C, Chen D L, Bhole S *et al*. *Materials Characterization*[J], 2009, 60(5): 370
12 Li Ying, Murr L E, McClure J C. *Scripta Materialia*[J], 1999, 40(9): 1041
13 Reynolds A P. *Scripta Materialia*[J], 2008, 58(5): 338
14 Pourahmad Pooya, Abbasi Mehrdad. *Transactions of Nonferrous Metals Society of China*[J], 2013, 23(5): 1253
15 Zienkiewicz O C. *International Journal for Numerical Methods in Engineering*[J], 1974, 8(1): 3
16 Sheppard T, Jackson A. *Material Science and Technology*[J], 1997, 13(3): 203
17 Sheppard T, Wright D S. *Metals Technology*[J], 1979, 6: 215
18 Sellars C M, Tegart W J M. *Acta Metallurgica*[J], 1966, 14(9): 1136
19 Yan Minggao, Liu Duopiao, Shi Changxu *et al*. *Handbook of Engineering Materials-Aluminum Alloy, Magnesium Alloy and Titanium Alloy*[M]. Beijing: Standard Press of China, 1989: 214 (in Chinese)
20 Midling O T, Grong O. *Acta Metallurgica et Materialia*[J], 1994, 42(5): 1595
21 Guerra M, Schmidt C, McClure J C *et al. Materials Characterization*[J], 2002, 49 (2): 95

Al/Mg 异种合金搅拌摩擦焊的材料流动可视化和数值模拟研究

宋 波[1]，翟洋洋[1]，左敦稳[2]，邓永芳[3]
(1. 兰州理工大学，甘肃 兰州 730050)
(2. 南京航空航天大学，江苏 南京 210016)
(3. 江西理工大学，江西 赣州 341000)

摘 要：采用切片法研究了搅拌摩擦焊接(FSW)接头的材料流动。通过对接头的三维重建，实现了流动材料的可视化，讨论了接头材料的流动模式和缺陷产生的原因。基于计算流体力学（CFD）和多相流理论，建立了 FSW 过程中铝合金/镁合金材料流动的三维数学模型。通过在数值模型中加入分布的示踪粒子，对不同连接参数下的材料流动模式进行分析和预测。结果表明：接头上部材料流动强烈，材料整体向前进侧迁移，接头中部前进侧镁合金向接头前部迁移，暂时形成的空腔由后退侧迁移来的铝合金填充。当不恰当的工艺参数使材料流动不充分时，未被完全填充的空腔会形成孔洞缺陷。接头材料整体主要以层流为主。在满足材料流动热输入需要时，接头材料的流动模式基本不发生改变，在高转速过热条件下，材料的迁移距离和混合模式会发生改变，2 种材料围绕搅拌头以层流模式多次越过对接线并充分混合，同时在后退侧产生紊流现象。

关键词：异种搅拌摩擦焊；2024铝合金；AZ31镁合金；材料流动；数值模拟

作者简介：宋 波，男，1983 年生，博士，讲师，兰州理工大学机电工程学院，甘肃 兰州 730050，E-mail: topsb1983@163.com